REPORT DOCUMENTATION PAGE

Form Approved
OMB No. 0704-0188

1. REPORT DATE *(DD-MM-YYYY)*	**2. REPORT TYPE**	**3. DATES COVERED** *(From - To)*
18-03-2010	Technical Paper	

4. TITLE AND SUBTITLE

Liquid Droplet Thrusters to Provide Constant Momentum Exchange Between Formation Flying Spacecraft

5a. CONTRACT NUMBER

5b. GRANT NUMBER

5c. PROGRAM ELEMENT NUMBER

6. AUTHOR(S)
Thomas B. Joslyn (AFIT); Andrew D. Ketsdever (AFRL/RZSA)

5d. PROJECT NUMBER

5f. WORK UNIT NUMBER
50260542

7. PERFORMING ORGANIZATION NAME(S) AND ADDRESS(ES)

Air Force Research Laboratory (AFMC)
AFRL/RZSA
10 E. Saturn Blvd.
Edwards AFB CA 93524-7680

8. PERFORMING ORGANIZATION REPORT NUMBER

AFRL-RZ-ED-TP-2010-099

9. SPONSORING / MONITORING AGENCY NAME(S) AND ADDRESS(ES)

Air Force Research Laboratory (AFMC)
AFRL/RZS
5 Pollux Drive
Edwards AFB CA 93524-7048

10. SPONSOR/MONITOR'S ACRONYM(S)

11. SPONSOR/MONITOR'S NUMBER(S)
AFRL-RZ-ED-TP-2010-099

12. DISTRIBUTION / AVAILABILITY STATEMENT

Approved for public release; distribution unlimited (PA #10159).

13. SUPPLEMENTARY NOTES
For presentation at the 57th JANNAF Joint Subcommittee Meeting, Colorado Springs, CO, 3-7 May 2010.

14. ABSTRACT

This paper presents the results of research on a novel concept in satellite propulsion that relies on momentum transfer through projection of silicon oil droplet streams through space. The system is useful to satellites flying side-by-side in formation that require a constant distance between them in order to conduct certain missions such as interferometric synthetic aperture radar observations. The force required to maintain separation is beyond what electric thrusters can provide without using large amounts power and significant amounts of propellant. Rational for selection of the silicone oil DC705 as the best working fluid is presented. Droplet size, velocity, and spacing needed for station keeping of various satellite mass and separation distance combinations is evaluated. Droplet streams of diameters demonstrated in this study and speeds demonstrated in past research can satisfy propulsion needs of satellites with masses in excess of 1000 kg in any earth orbit. A droplet stream system requires an order of magnitude less mass than comparable electric propulsion systems and two orders of magnitude less power and is an enabling technology for side-by-side formation flying. Environmental impediments to collection of droplets transiting between satellites were analyzed and three significant obstacles identified; atmospheric drag, droplet freezing, and Lorentz forces due to droplet charging.

15. SUBJECT TERMS

16. SECURITY CLASSIFICATION OF:			**17. LIMITATION OF ABSTRACT**	**18. NUMBER OF PAGES**	**19a. NAME OF RESPONSIBLE PERSON**
					Dr. Andrew Ketsdever
a. REPORT	**b. ABSTRACT**	**c. THIS PAGE**			**19b. TELEPHONE NUMBER** *(include area code)*
Unclassified	**Unclassified**	**Unclassified**	SAR	26	N/A

Liquid Droplet Thrusters to Provide Constant Momentum Exchange Between Formation Flying Spacecraft

Thomas B. Joslyn[i]
US Air Force Academy, Colorado Springs, CO 80841

Andrew D. Ketsdever[ii]
Air Force Research Laboratory, Propulsion Directorate, Edwards AFB, CA 93524

This paper presents the results of research on a novel concept in satellite propulsion that relies on momentum transfer through projection of silicon oil droplet streams through space. The system is useful to satellites flying side-by-side in formation that require a constant distance between them in order to conduct certain missions such as interferometric synthetic aperture radar observations. The force required to maintain separation is beyond what electric thrusters can provide without using large amounts power and significant amounts of propellant. Rational for selection of the silicone oil DC705 as the best working fluid is presented. Droplet size, velocity, and spacing needed for station keeping of various satellite mass and separation distance combinations is evaluated. Droplet streams of diameters demonstrated in this study and speeds demonstrated in past research can satisfy propulsion needs of satellites with masses in excess of 1000 kg in any earth orbit. A droplet stream system requires an order of magnitude less mass than comparable electric propulsion systems and two orders of magnitude less power and is an enabling technology for side-by-side formation flying. Environmental impediments to collection of droplets transiting between satellites were analyzed and three significant obstacles identified; atmospheric drag, droplet freezing, and Lorentz forces due to droplet charging.

---

[i] Assistant Professor, Department of Astronautics, U.S. Air Force Academy, Colorado Springs, CO 80841
[ii] Senior Research Engineer, Aerophysics Branch, 10 E. Saturn Blvd., Edwards AFB, CA 93524

Nomenclature

C	=	capacitance
e	=	electron elementary charge
E_{photon}	=	incident photon energy
E_{gauss}	=	fontheim distribution constant derived empirically from satellite observations
F_c	=	Coulomb forcesQ_1 Q_2))/(r_sep^2)
$F_{surf\ tension}$	=	Surface tension force
I_e	=	incident electron current on the surface
I_i	=	the incident ion current
I_{se}	=	secondary electron current caused by incident electrons
I_{si}	=	secondary electron current caused by incident ions
I_{bse}	=	current from a surface due to backscattered incident electrons
I_{ph}	=	secondary electron current caused by incident photons.
$\vec{J}$	=	incident current density at the surface
L	=	rate of recombination
m_e	=	mass of an electron
n	=	charged particle number density
n_e	=	the local electron density (m^{-3})
n_i	=	the local ion density (m-3).
Q	=	ionization rate, droplet total charge
r	=	droplet radius (m)
T_{surf}	=	surface tension coefficient (0.0365 N/m for DC705)
V	=	voltage potential
V_o	=	electrostatic voltage
$\vec{v}$	=	bulk flow velocity
Y	=	yield ratio of electrons released to photons absorbed
θ	=	low-energy ionospheric plasma temperature
$\theta_{maxwellian}$	=	Fontheim distribution constant derived empirically from satellite observations
ζ	=	Fontheim distribution constant derived empirically from satellite observations
Δ	=	Fontheim distribution constant derived empirically from satellite observations
ϵ_0	=	the permittivity constant of free space
ϕ	=	the local charge potential (Volts)
ρ	=	charge density
κ	=	dielectric constant specific to a material
ψ_{sun}	=	photon incidence angle to droplet surface

I. Introduction

The research presented here evaluates momentum exchange through fluid streams as a means of maintaining side-by-side spacing between a pair of formation satellites. Droplet streams of very low vapor pressure silicone oil are generated on each spacecraft and projected through space to a receiving satellite. The receiving satellite collects the droplet stream and pumps the fluid to heat exchangers on warm spacecraft components removing heat from those components while warming the fluid. Fluid is pressurized further in a droplet generator where a return stream is produced and sent back to the originating satellite to begin the process again. The concept might look like Figure 1 in which two spacecraft are travelling in the horizontal direction while imaging the Earth.

Figure 1. Droplet Stream Propulsion Concept in which Momentum is Exchanged Between Satellites Creating a Continuous Displacement Force that Maintains separation from the Reference Orbit Centerline.

The side-by-side satellites use streams of small silicon oil droplets continuously exchanged to produce the force needed to maintain constant separation. This study investigated various aspects of generating and collecting such a droplet stream including the many environmental forces acting to disturb droplets from their intended path between satellites. These forces include drag, solar radiation pressure, Lorentz forces, and electrostatic interactions between droplets. Predictions of plasma and ultraviolet radiation charging of droplets are needed in order to quantify Lorentz forces accurately. A material charging model called NASCAP was used to predict droplet charge levels and the ultraviolet radiation induced charging was validated experimentally in vacuum.

A. Motivation for Tandem Satellites

In the past decade, the advantage of satellite formations to the field of remote sensing gave rise to several proposals for their implementation. The first tandem satellite formation to fly will likely be a satellite pair called TarraSAR and Tandem-X. TarraSAR is in orbit, operated by the German Space Agency and Tandem-X is expected to be launched in 2010. These satellites will provide the first bi-static synthetic aperture radar (SAR) platform in space. This technique is expected to provide topographic imaging resolution on the order of 1cm.[1]

To achieve a side-by-side configuration, the Tandem-X formation utilizes two offset polar orbits depicted in Figure 2. Because of the ever-changing TanDEM-X separation distance, the formation is ill-suited for uniform observations of the Earth because is unable to achieve the same separation baseline over all parts of the Earth. Such consistency of baseline is necessary for consistent coverage of the entire Earth and for timely detection of surface changes.

Since tandem, side-by-side satellites are each in orbits around the center of the Earth their orbits cross twice every orbital period and they tend to converge on each other unless a continuous separation force counteracts this convergence. The magnitude of the separation force required is proportional to the total mass of the two spacecraft and their separation distance. Applying the Clohessy-Wilshire equations, Tragesser[2] has quantified this force as a function of spacecraft mass and separation distances. In GEO, the thrust force is 20 to 100 mN for satellites between 100 and 1000 kilograms with 1km spacing. In LEO, 100 to 1000 mN is required for the same satellite masses and separation distances.

A range of formation separation distances between tens of meters to at least one kilometer is useful to the remote sensing community.[3] In this study, droplet diameters were produced that are capable of providing several Newtons of thrust when travelling at stream velocities demonstrated in past droplet stream studies.[4] Such streams generate the necessary momentum transfer with a single pair of droplet streams to provide two 3000 kg LEO satellites with one kilometer separation.

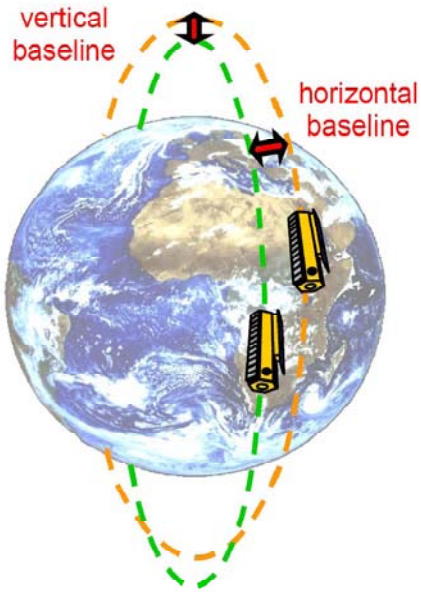

Figure 2. Tandem X Formation Orbit Configuration Providing Various Baseline Distances from which Interferometric Synthetic Aperture Radar will be Performed in 2010.

Polar orbit is both a desirable place to fly remote sensing satellites in formation and a challenging environment to perform droplet transfer due to dramatic changes to the auroral plasma charging environment during periods of high geomagnetic activity. The focus of this study is on obstacles to using the concept in GEO, LEO, and polar orbit. This study focuses on the effects of these very different plasma-charging environments on droplet transport. In this study, uniform droplet streams with diameters of up to 1.5mm were produced with velocities in the 5m/s range and a frequency of approximately 0.5 Hz. Individual droplets with consistent diameters as large as 3.5mm were produced in vacuum for this study. An increase to 5mm at 50m/s expands allowable spacecraft mass beyond 6000 kg with 1km separation in LEO.

B. Fluid Selection and Droplet Generation

Droplet streams in space were first proposed in the 1980s to facilitate the radiation of waste heat on large space structures like power generating satellites and the space station. The National Aviation and Space Administration (NASA) and the Air Force (USAF) funded the Liquid Droplet Radiator (LDR) program that demonstrated feasibility of droplet streams and developed technologies for generating and collecting them in space. More than two dozen articles in the literature describe the formation and use of droplet streams in the space environment. Of note, is work done in the 1980s by researchers at the University of Washington,[5] the University of Southern California (USC)[6], NASA's Glenn Research Center and Air Force Research Laboratory (AFRL).[7] NASA and the USAF funded studies by several contractors that resulted in proven technologies for fluid stream generation and collection. NASA researchers successfully tested LDR components in drop tower free fall conditions.[8] Many of the technologies developed for the LDR program would be equally useful for droplet stream propulsion.

Many types of low vapor pressure fluids were considered for use in a droplet stream propulsion system. LDR researchers considered the fluids in Table 1 and the fluid selected by NASA and the USAF in the 1980s was trimethyl pentaphenyl siloxane which is a silicone based oil known best by its trade name Dow Corning 705 (DC705).**Error! Bookmark not defined.** This fluid has a low vapor pressure and relatively low viscosity at nominal satellite operating temperatures. DC705 continues to be the working fluid of choice for more recent LDR designs and was selected for LDR testing performed by Japanese researchers as recently as 2005.[9]

Table 1. Candidate Fluids and their Properties at 20°C. Error! Bookmark not defined.

Fluid	Vapor Pressure (Torr)	Molecular Weight (amu)	Viscosity (centistokes)
DC705	$3x10^{-10}$	546	175
DC704	$2x10^{-8}$	532	39
Neovac SY	$1x10^{-8}$	634	40

Low viscosity is advantageous because it allows droplet stream production at a lower reservoir pressure. Other fluids considered include another silicone oil called DC704 and a synthetic hydrocarbon called Neovac SY. Both fluids are desirable for their relatively low viscosity, and low vapor pressure.

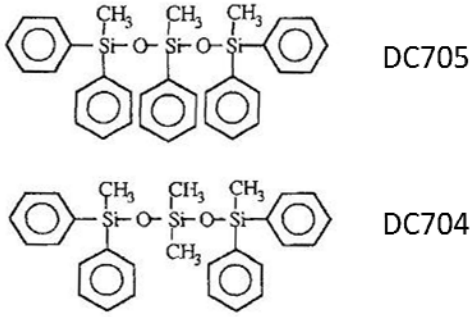

Figure 3. DC705 and DC704 Molecules Chemical Structure wherein Hexagon Rings represent Benzene Rings: C_6H_6 (From Koizumi, 1996).

DC704 and DC705 have similar density; 1070 kg/m^3 for DC704 and 1097 kg/m^3 for DC705. The fluids differ chemically by a single methyl group, which is replaced by a fifth Benzene ring (C_6H_6) in DC705 as seen in **Error! Reference source not found.**. Previous research shows that charging properties of DC704 and DC705 are very similar.[10] For these reasons, much of the research presented in this report is quite applicable to both DC704 and DC705. In fact, DC704 was used as a less expensive alternative for some charging experiments performed in support of this research.

As seen in Figure 4, the vapor pressure of silicone oils, and other fluids considered, increases significantly as a function of temperature. As a result, DC705 is only practical for use at temperatures below 350K. For most spacecraft, this temperature limit is quite reasonable since it is rare for spacecraft components to require operation at temperatures exceeding 350K. Indeed, one of the advantages of having fluid on-board is the flexible temperature control it affords the spacecraft through active control of fluid flow and by using the propulsion system itself as a liquid droplet radiator.

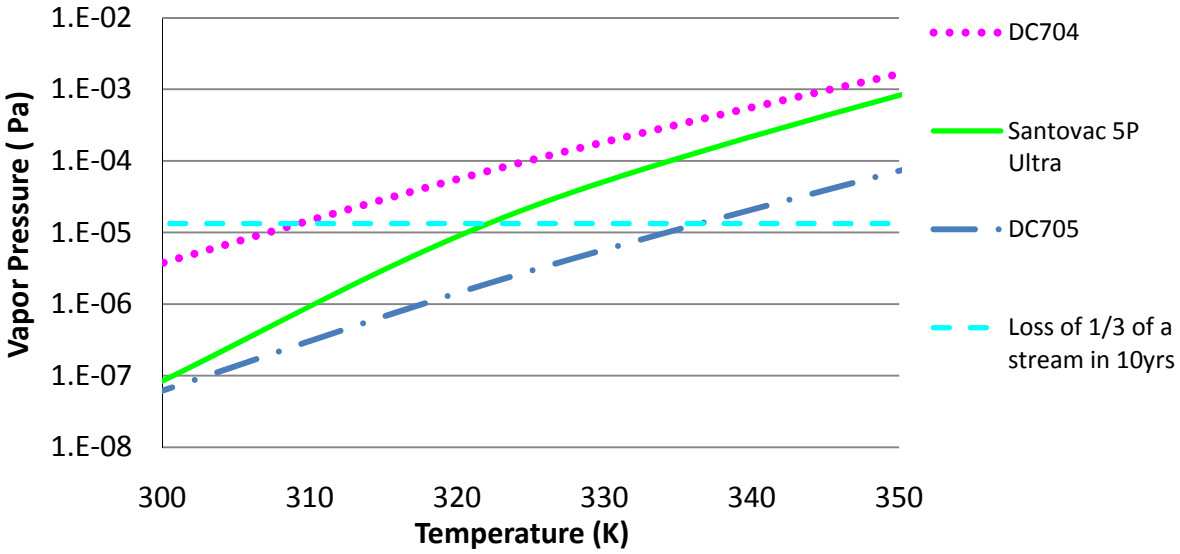

Figure 4. Vapor Pressures of Fluid Candidates Versus Temperature where a Vapor Pressure of $1.0x10^{-5}$ results in Loss of 1/3 of the Mass of a Stream in 10 Years.

It is necessary to break up a fluid column into uniform droplets to prevent randomly sized droplets from forming

due to the tendency for a fluid column to minimize its surface area. This phenomenon, called Rayleigh instability, causes breakup into droplets of random size at about 3 stream diameters from the producing orifice.[11] Droplets of varying size are affected differently by drag and other forces described in this study resulting in a very large impact region at the receiving satellite, making collection difficult. Droplet generators developed for the LDR program were based on vibration-induced breakup of a fluid column in to droplets. This mature technology was first pioneered by Lord Rayleigh in the 19th century.[6]

Micro solenoid valves are a proposed new method of droplet generation. This technology was developed in the decade following NASA and USAF cancellation of the LDR program and these valves are currently used in many vacuum applications in space. These valves can operate for several million cycles and are capable of generating a droplet stream for 3-5 years. Two types of micro solenoid valves were tested in this study and were found to produce droplet streams of sufficient uniformity, size, and speed to satisfy requirements of systems envisioned. When compared to piezoelectric droplet generators, solenoid generators have less fluid loss at startup and shutdown and can produce droplets with any desired gap distance between droplets. Larger gaps between droplets reduce electric field strength between droplets that would otherwise cause dispersion of transiting droplets from the direct path between satellites.

C. System Performance and Comparison with Ion Engines

GEO satellite propulsion needs are low and can be satisfied by a single opposing pair of droplet streams using already proven stream size and velocity. Droplet streams of demonstrated size and speed extended over a 1km distance require less than 100mL of silicone oil in transit at any one time. The need for additional fluid beyond that which is in transit will be discussed later but, even after accounting for expected fluid loss and extra fluid needed to ensure correct collector and pump operation, the impact of fluid propulsion on a typical GEO satellite's mass budget is less than 2% of system mass.

In LEO where the propulsion need is much greater, the need for larger droplet diameters results in a need for more fluid in transit. Droplet stream speed has a significant effect on the amount of fluid in transit because slower droplets spend more time in transit and because slower speeds require more fluid mass to provide the required momentum exchange. A transit velocity of only 10m/s requires about 5 liters of fluid in transit to maintain 1km spacing of 500kg satellites whereas a transit velocity of 50m/s has about 70 ml of fluid in transit.[13]

Additional fluid is required in feed lines and to account for evaporation losses. The amount of fluid needed on each satellite is roughly equal to 3 times the amount of fluid in transit. About 9kg of DC705 is needed to maintain 1km separation of two 500kg satellites in LEO with a transit speed of 20m/s. This represents less than 2% of the total spacecraft mass and displaces some mass otherwise needed for a conventional thermal control system (TCS). Based on the mass of components developed for the LDR program[12] it is estimated that a droplet stream propulsion system for LEO satellites will require less than 6% of a spacecraft's mass budget. Moreover, when additional radiating streams are collected, a droplet stream system can remove as much heat as conventional radiators weighing three times as much.[13]

Low thrust propulsion to maintain a tandem spacecraft formation can be provided by ion engines or other forms of electric propulsion. Ion engines operate with a specific impulse (Isp) on the order of 6000 seconds. An EADS Astrium RIT-22 ion thruster consumes three orders of magnitude more propellant mass than a 50m/s stream system loses to conservative estimates of evaporation.[13] In terms of fluid evaporated, the Isp for a 3mm, 50m/s stream is on the order of 9 million seconds and the efficiencies of faster and larger streams are even higher.

In addition to specific impulse, system mass was analyzed to properly compare ion thrusters with droplet stream systems. LDR system components applicable to droplet stream propulsion include fluid pumps, collector structure, reservoir, feed lines, heat exchangers, flow directing valves and droplet generator solenoid valves. In addition, a pointing platform may be required for the droplet generator unless satellite attitude control systems can ensure stream pointing accuracy. A first order approximation of system dry mass of 10-20kg was calculated using component masses reported by NASA and AFRL.[7] By comparison a RIT-22 Ion thruster weighs 7kg (dry mass) and six of them are required on each satellite to provide the same thrust provided by opposing 2mm, 50m/s droplet streams.[14]

Droplet streams have a decided advantage over electric propulsion is in the areas of operating power. A single RIT-22 consumes over 5kW of power whereas a droplet stream system, providing the same thrust as six RIT-22 engines, is estimated to use less than 50W. For most satellites, this two order of magnitude disparity in continuous required power is more significant than a 5-fold mass savings and puts droplet stream propulsion in its own class. Figure 5 compares the performance of existing electric propulsion systems used currently used in orbit. Droplet

stream propulsion is literally off the chart in both axes with power requirements below 100 Watts and specific impulse in the millions.

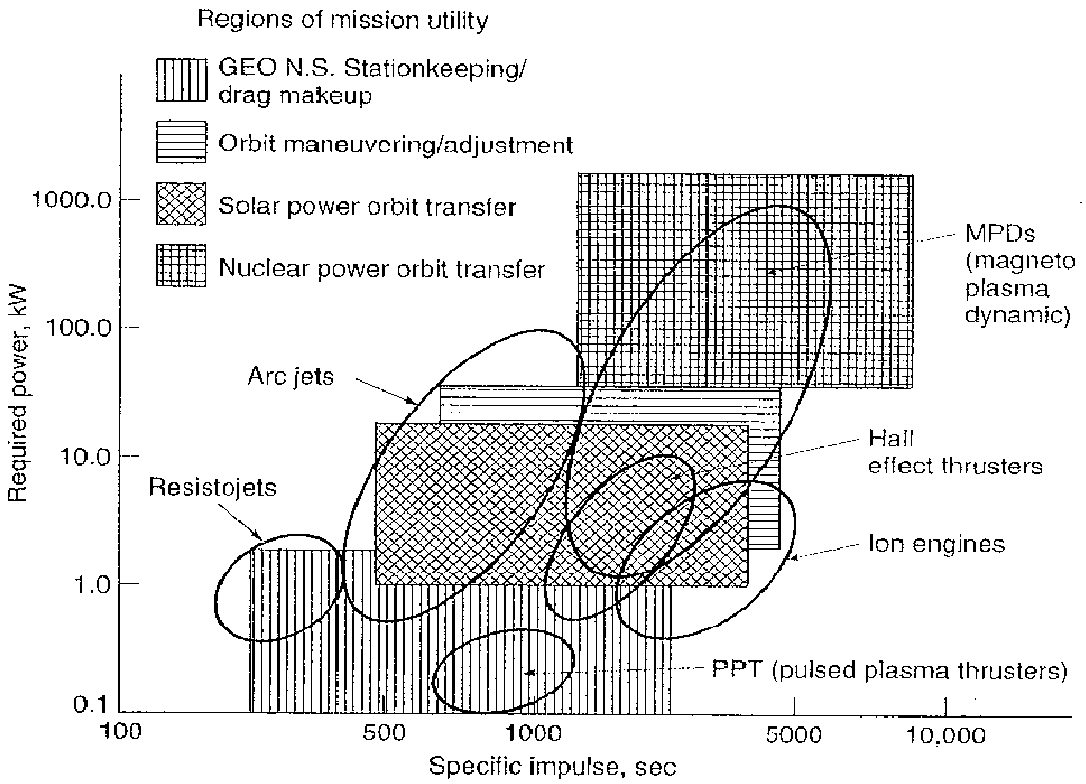

Figure 5. Power and Specific Impulse of Various Electric Propulsion Systems Currently Used in 4 Missions, Each with a Different Range of Required Power and Specific Impulse. Droplet Stream Propulsion has Specific Impulse greater than 600,000 seconds and Power Requirements of Less than 0.05 kW (from Sutton, 2003).

II. Environmental Impacts on Droplet Streams

As droplets travel between satellites, they are exposed to the near Earth environment which affects the path that the droplets follow and the chemical makeup of the droplet material itself. Solar pressure forces are negligible at all altitudes and result in off-course droplet drift of less than a few millimeters.[13] Atmospheric drag is a

A. Drag and Heat Transfer

Drag is significant below 600km and slows droplet orbital velocity much more than it does the orbit velocity of satellites. In this way, drag alters the trajectory of transiting droplets and can result in droplets straying 10cm or more from a direct path between satellites.[13] Increasing the size or density of droplets helps reduce the magnitude of drift due to drag. The direction and magnitude of drag force is relatively predictable and can be compensated for by projecting a stream that leads the target collector sufficiently. A droplet stream pointing control system will require a feedback sensor that can detect droplet impact location. A prototype of such a device was developed and tested in this study and demonstrated that charged fluid filling the gap between two wire mesh pieces causes a measurable change in capacitance.[13] An array of such wire mesh pieces inside of a droplet stream collector could provide impact location feedback information.

Heat transfer within a droplet via conduction is significantly faster than radiation of heat from the surface. Analysis shows that surface radiation is slow enough that droplets 1mm in diameter will not freeze during transits of several kilometers at reasonable speeds (20m/s). Larger or faster droplets can travel even further without freezing and droplets only freeze in eclipse.[13] Heat loss through radiation by transiting droplets is useful to most satellites that

have excess heat, even in eclipse. Droplet streams will reduce or eliminate the need for traditional radiator systems to control on-board temperatures and typically require less than half of the mass of traditional radiator systems.[13]

Radiation and atomic oxygen may damage the molecular structure of the fluid and could lead to changes in viscosity, electromagnetic energy absorption, bulk conductivity, and possibly other properties. A study of the effects on DC705 of exposure to charged particles was accomplished for the LDR program in the 1980s. DC705 was exposed to positive ions for more than 72 hours which resulted in some discoloration and indications of the presence of aromatic compounds.[15] Further study of charged particle exposure of silicone oils is warranted. In the current study, DC705 samples were exposed to ionizing levels of EUV light and then analyzed using infrared spectroscopy. Samples exposed to EUV for 15 and 30 minutes showed no chemical changes in the fluid.

B. Relevance of Droplet Charging to Droplet Stream Propulsion

Once the utility of droplet stream momentum transfer was established and the more obvious impediments to its implementation quantified, the focus of this study turned to the issue of droplet charging in space. Exposure to the plasma and radiation environment of space results in negative or positive charging of transiting droplets. Charging is a concern for the following reasons:

- Charged droplets will experience Lorentz forces associated with interaction with Earth's magnetic field.
- Electric fields between charged droplets will cause droplets to repel one another, which alters their trajectory between satellites.
- If droplet charge gets high enough, it will cause droplets to break up into smaller droplets of various diameters and with trajectories altered from that of the original droplet.

One of the more likely missions to employ droplet stream propulsion is remote sensing. These spacecraft will likely utilize a polar orbit in order to provide global coverage. The environment in polar orbit differs significantly from that of lower inclination LEO because of the influx of high-energy plasma is channeled by the magnetic field toward the Earth. Auroral electrons typically have energy levels of several keV, and are capable of more severe charging than the electrons encountered at lower latitudes. Objects in polar orbit encounter these annular regions above the geomagnetic poles for very short durations four times each orbit. Droplets that transit between satellites in auroral space will experience a much stronger plasma charging environment than droplets transiting at lower latitudes.

Charging of droplets at LEO altitudes differs significantly from charging in GEO because of the large population of low energy plasma subject to attraction or repulsion by a charged object.[13] Droplet charging in low latitude LEO was estimated by analytic and numerical methods that show it is a rather benign charging environment relative to GEO or auroral space. Thus, in this study, emphasis was placed on accurately predicting nominal and peak charging encountered by polar orbiting droplet streams. The auroral regions, like the rest of LEO, contain neutral particles and low energy ions from the atmosphere. However, the auroral zones also contain a significant population of high-energy plasma particles, particularly during periods of high geomagnetic activity.[13] The composition of this ever-changing plasma environment is more complex, though less extreme, than the geosynchronous environment. As a result, energy flux distributions that characterize the ambient plasma populations in the auroral regions are more complex than those used to predict the charging environment in low latitude LEO and GEO.

To characterize the flux of particles in the orbit environment affecting a droplet it is necessary to determine a number density and particle velocity probability distribution. The time rate of change of charged particles into the volume of space surrounding a droplet is proportional to the net flow of particles into and out of the volume and the production (ionization) and loss (recombination) of charged particles. Mathematically, this is described by the following equation where n is the charge particle number density, v is the bulk flow velocity, Q is the ionization rate, and L is the rate of recombination.[16]

$$\boldsymbol{dn}/_{\boldsymbol{dt}} = (-\boldsymbol{\nabla} \boldsymbol{n}\vec{\boldsymbol{v}}) + \boldsymbol{Q} - \boldsymbol{L} \tag{1}$$

In non-polar LEO, the ambient low energy plasma is in thermal equilibrium and $\mathrm{dn}/_{\mathrm{dt}}$ is equal to zero, and the normalized probability distribution can be accurately (to a first order) described by a Maxwellian distribution.[16] In the Auroral portion of a polar orbit, electron velocity distribution is more complex and is not described accurately by a Maxwellian distribution. **Error! Reference source not found.** shows a comparison of actual levels of electron flux densities recorded by spacecraft passing through the auroral region. The figure also shows Fontheim curve fits to the data that accurately describe the flux density as a

function of particle energy. A Fontheim distribution is described by the superposition of four terms defined in the following equation where n is density of the low-energy ionospheric plasma, e is electron elementary charge, m_e is the mass of an electron, and θ is the temperature of the low-energy ionospheric plasma.

$$Flux(E) = \overbrace{\sqrt{\frac{e}{2\pi\theta m_e}}\frac{E}{\theta} n\, exp\left(-\frac{E}{\theta}\right)}^{\text{Term 1}} + \overbrace{\pi\zeta_{max} E\, exp\left(-\frac{E}{\theta_{max}}\right)}^{\text{Term 2}} + \overbrace{\pi\zeta_{gauss} E\, exp\left[-\left(\frac{E_{gauss}-E}{\Delta}\right)^2\right]}^{\text{Term 3}} + \overbrace{\pi\zeta_{power} E^{-\alpha}}^{\text{Term 4}} \quad (2)$$

The various ζ terms, as well as θ_{max}, E_{gauss} and Δ are constants derived empirically from satellite observations. The power law exponent, α, in term four, describes low energy electron flux during high geomagnetic activity. The flux density calculated using the Fontheim distribution equation has the units $(eV\ ster\ m^2)^{-1}$. A parametric analysis determined that the Fontheim component with the greatest impact on maximum surface potential (by at least a factor of 3) was the Gaussian term. This knowledge was used to select the Fontheim fits to satellite observed auroral data most likely to result in high levels of droplet charging.[13]

Three charged particle distribution models of GEO environments were used in this study. The first two of these models are defined by NASA-TP-23613 and are known as NASA worst-case GEO charging environments. These worst-case environments are single and double Maxwellian distribution fits to SCATHA and ATS-6 satellite data. Both distributions provide a high flux of high-energy electrons capable of charging certain spacecraft materials to some of the largest negative potentials ever seen.[17] These distributions constitute the worst-case NASA design guidelines specified by Purvis et al,[17] in 1984 and revised by JPL scientists in 2005.[17] These guidelines have remained the standard for surface electrostatic charging among U.S. spacecraft designers for over two decades.[18] The last plasma distribution in Table 2 is a nominal GEO charging environment. This nominal environment represents average GEO environment conditions as reported by the SCATHA and ATS-6 spacecraft.

Table 2. GEO Charging Environments Used in this Study.

Environmental	NASA Worst-	NASA Worst-	Nominal GEO
Distribution	Single	Double	Double
Electron Density (m^{-3})	$1.1x10^6$	$1.2x10^6$	$7x10^5$; $2.25x10^5$
Electron Temperature	$1.2x10^4$	$1.6x10^4$; 1000	400; 8200
Ion Density (m^{-3})	$2.4x10^5$	$2.4x10^4$; 8820	$6x10^5$; $4x10^5$
Ion Temperature (eV)	$2.95x10^4$	$2.95x10^4$; 111	450; $1.9x10^4$
Electron Current (A/m^2)	$3.3x10^{-6}$	$4.1x10^{-6}$	$9.6x10^{-7}$
Ion Current (A/m^2)	$2.5x10^{-8}$	$2.5x10^{-8}$	$2.2x10^{-8}$

C. Droplet Charging Theory

As silicon oil droplets move through space they come into contact with ambient electrons and ions from the sun and Earth's atmosphere that constitute the plasma environment of space. Free electrons in near-earth space move in all directions at very high speeds that are about 200km/s, more than an order of magnitude higher than orbital velocities. Consequently, electrons impact orbiting bodies from all directions as depicted in Figure 6. In contrast, positively charged ions in near-earth space have an average velocity magnitude ($\bar{v}$) of only about 1km/s. This is significantly slower than orbit velocity, and ions tend to hit the ram side of orbiting bodies much more frequently than the wake side. The velocity of electrons is about two orders of magnitude greater than that of ions and the resulting flux of electrons to the surface is up to 50 times greater than the flux of ions to the surface.[21] Because electrons have a flux rate so much higher than that of ions they tend to play a more significant role in determining the charge of materials in space than ions do.

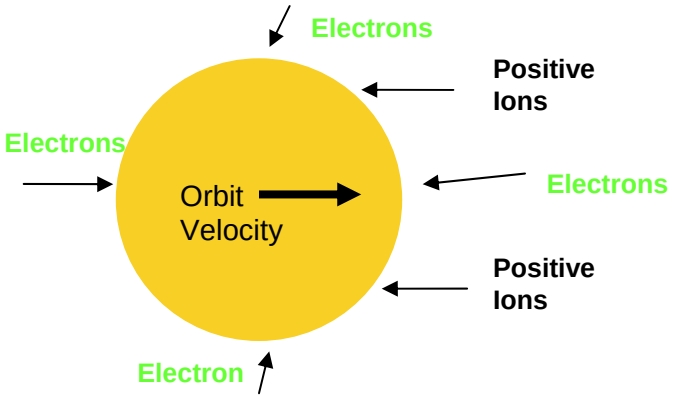

Figure 6. Charging Sources in the Space Plasma Environment.

Atoms near a droplet's surface absorb low energy electrons and materials in LEO and Polar orbit tend to charge negatively under nominal geomagnetic conditions when incident electron energies are low. As the surface material is charged, a plasma sheath forms around the object and Coulomb repulsion forces become sufficient to reflect some inbound electrons. As a result, negative charging of spacecraft materials (and silicon oil droplets) in LEO due to plasma is limited to just a few volts, even during periods of high geomagnetic activity.[19] The presence of low energy (cool) atmospheric plasma in LEO and Polar orbits has a similar charge limiting effect for objects that are charged positively by secondary electron production or photoemission of electrons at the surface. As the surface charges positively, electron deposition rates increase as fewer electrons are reflected.

A droplet in the ambient space plasma acts like an isolated electrical probe. As such, it adopts an electrostatic potential consistent with charge collection as modeled by Maxwell's equations.[20] Hastings and Garret[21] have shown that the divergence of the Poisson equation and Ampere's law yield the following relationship for a sphere in a space plasma environment:

$$\frac{\partial \rho}{\partial t} + \nabla \cdot \vec{j} = 0 \tag{3}$$

Here ρ is the charge density and $\vec{j}$ is the incident current density at the object's surface. Integrating over the space outside of the sphere and applying the divergence theorem yields:

$$\frac{\partial Q}{\partial t} = I_{net} \tag{4}$$

Here Q is the total charge of the sphere (in Coulombs) and I_{net} is the net current at the surface. To determine the charge of an object immersed in a plasma it is necessary to solve the net current equation while simultaneously solving Poisson's equation for charge density where ϵ_0 is the permittivity constant of free space, ϕ is the local charge potential (Volts), e is the charge of an electron in Coulombs, n_e is the local electron density (in m-3), and n_i is the local ion density (m-3).[21]

$$-\rho = \epsilon_0 \nabla^2 \phi = e(n_i - n_e) \tag{5}$$

An object in space is exposed to many different processes that add or remove electrons at the surface. Determining the net current at the surface of an object is a matter of determining and then summing the current due to each of these processes. Quantifying net current is complicated by the fact that the processes that add or remove electrons from the surface are also influenced by the surface charge. Secondary electrons with sufficient kinetic energy to escape in one instant may be retained by a more positively charged surface in the next. Consequently, the most accurate charge determination algorithms are iterative, solving for the charge density and potential of the elements of a mesh of small volumes for a time step and then repeating the process for the next time step. Mathematically, the current balance for a droplet at a floating electrostatic potential (V) is expressed by the following equation:[22]

$$I_{net}(V) = I_e(V) - [I_i(V) + I_{se}(V) + I_{si}(V) + I_{bse}(V) + I_{ph}(V)] \quad (6)$$

Here I_e is the incident electron current on the surface, Ii is the incident ion current, Ise is the secondary electron current caused by the incident electrons, Isi is the secondary electron current caused by the incident ions, Ibse is the backscattered incident electrons, and Iph is the secondary electron current caused by incident photons.

Each of the terms inside the square brackets in the net current equation represents a process that removes electrons from the object or, much less frequently, adds positive ions to the object. Terms inside the brackets reduce current flow to the object and result in negative (or less positive) charging of the material. Processes that result in positive charging are principally caused by the removal of electrons from atoms in the surface material by energetic particles or photons entering the surface. An electron or ion entering a material with an energy state above the material's ionization potential may produce one or more secondary electrons. An inbound electron is slowed through random elastic collisions with nuclei and penetrates a certain distance into the droplet. When an electron is slowed sufficiently, Coulomb force interaction with other electrons bound to atoms within the material may liberate those electrons from their parent atoms. These free electrons are called secondary electrons.

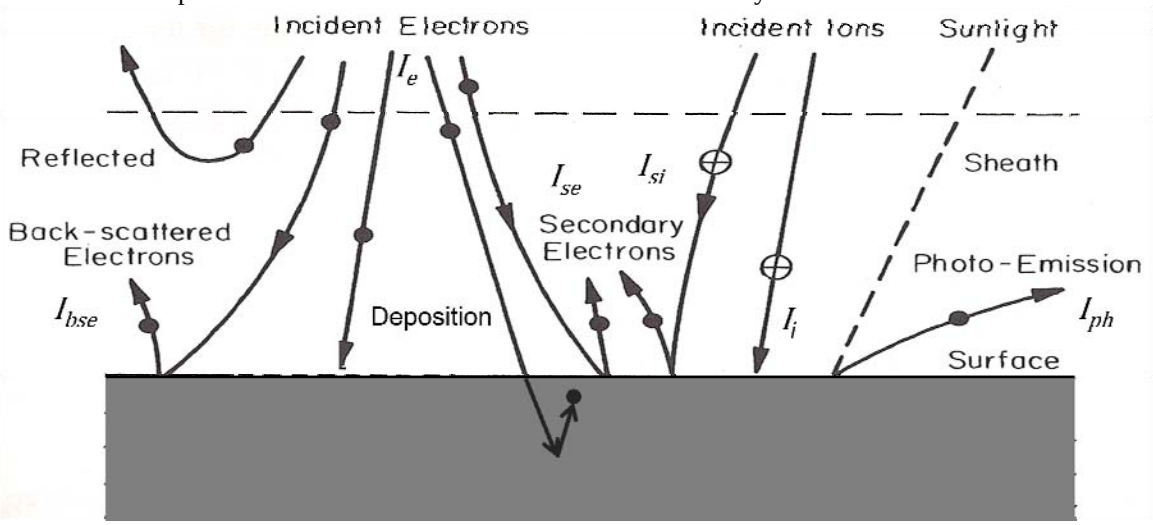

Figure 7. Charging Processes at the Surface of a Dielectric Material (after Hastings, 1996).

Secondary electrons may escape the material, be conducted by the material, or be absorbed by other atoms in the material depending on the energy state of the secondary and on material properties discussed. Incident ions and photons of sufficient energy can also produce secondary electrons. These sources of secondaries are generally less significant than incident electrons but their impact on DC705 charging is accounted for by NASCAP simulations. Figure 7 provides an overview of the various processes that result from the impact of charged particles or photons at the surface of a dielectric material. As the surface charge increases, low energy electrons or ions can be reflected, reducing the rate of plasma deposition.

Electrons can also be backscattered by interaction with atomic nuclei so that the electron's trajectory is changed without much energy loss and the electron escapes the material. Capture of low energy electrons by atoms in the material, called deposition, results in negative material charging. High-energy electron impacts can result in a net negative or net positive charge on an object.

The total secondary yield of electrons from a surface, δ, is defined as the average number of emitted electrons produced by the surface per incident electron. This total yield is composed of true secondary electrons, δ_t, and backscattered electrons, η, as in the following equation: $\delta = \delta_t + \eta$. The backscattering rate, η, is the average number of incident electrons scattered from the surface. Essentially, these electrons are reflected from the surface and leave the surface with more energy than true secondary electrons. Backscattered electrons have an energy distribution that is usually peaked close to the primary incident energy and most of these electrons have an energy state of more than 50eV. Experiments done to determine true secondary yield rates for DC705 caused by incident electrons were found in the literature and are presented later.

High-energy photons from the sun play a role in charging DC705 droplets because of their ability to couple with electrons. If photon energy is sufficient (at least 7.2eV for DC705) there is a certain probability that the photon will impart enough energy to liberate an electron within an atom of the material. This process is the photoelectric effect

and results in photoemission of electrons called photoelectrons. For Earth orbiting spacecraft, the current due to photoemissions is generally 10-40 $\mu A/m^2$ and is usually less significant than other sources of secondary electrons, particularly in GEO and auroral space.[21]

The first particles to affect a newly formed droplet exposed to the sun are solar photons travelling at the speed of light. Photons above the electron binding energy for DC705 give the droplet a positive surface charge by liberating photoelectrons from the material. This initial positive charge due to photoemissions is followed by low energy electron deposition inducing a negative charge and secondary electron production producing a positive charge. The charged surface attracts oppositely charged particles from the surrounding plasma and the first layer of a plasma sheath is formed. This layer, in turn, attracts particles from the ambient plasma with charge opposite that of the first layer. In this manner, the sheath grows and dampens the surface potential until it reaches a thickness at which the surface potential is completely shielded and has zero potential relative to the ambient plasma.

Droplet orbital velocity determines which side of the droplet is exposed to positive ions. In LEO, below about 650km, most ions are atomic oxygen atoms ionized by solar EUV radiation. Above 1000km protons are the dominant ion species, and ions in GEO are almost exclusively protons.[21] In LEO, the droplet's orbital velocity is greater than that of most ambient ions. Because of this, most ion impacts occur on the leading hemispheric surface. Electron velocities are more than an order of magnitude greater than orbital velocities and therefore electron impacts occur nearly uniformly around the droplet's spherical surface. Distribution of differential hemispheric charge is limited because DC705 is a relatively poor conductor. The various effects acting on a droplet that is moving perpendicular to the sunward direction are summarized in Figure 8 where the processes that are typically the most significant are in bold text:

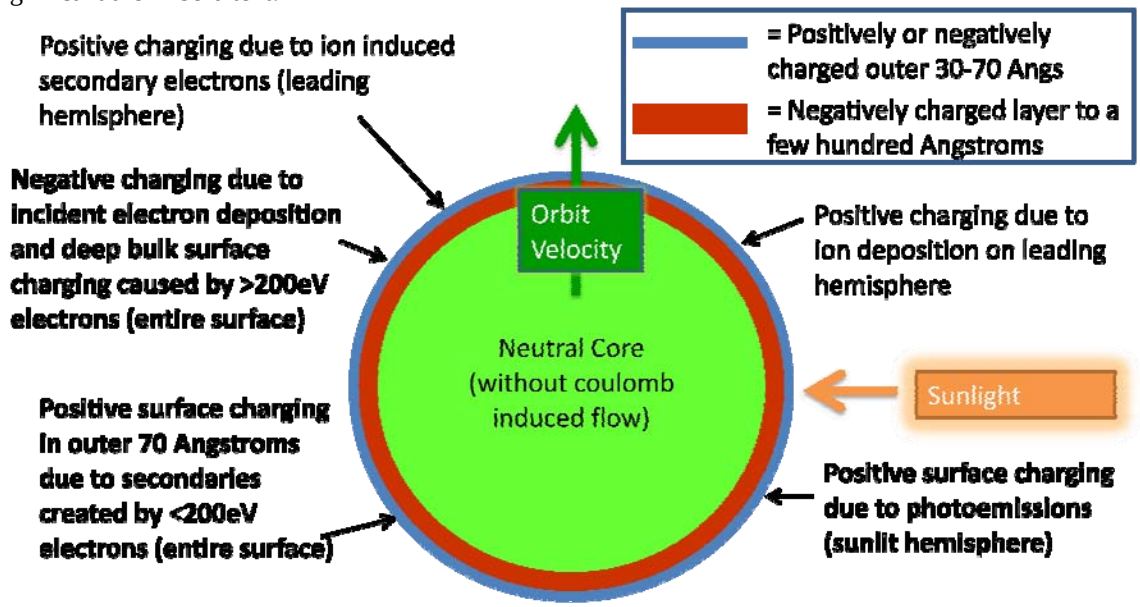

Figure 8. Charging Processes Affecting DC705 Droplets.

The fact that DC705 is a liquid allows for movement of charged molecules within the fluid sphere. Positively charged molecules in the outer layer are attracted to underlying negatively charged molecules, which can lead to mixing of ions in the charged outer region of the droplet. If such mixing occurs on time scales below the transit time of droplets, the result will be a relatively uniform distribution of charge over the entire droplet surface. In sunlit droplets Coulomb forces may also induce fluidic flow from the sunlit side to the more negatively charged shaded side.

In LEO, charged particles from the sun are, on average, much more energetic than particles from the Earth's upper atmosphere and are more likely to ionize surface materials. Unlike neutral particles, charged particles are influenced by electromagnetic fields that are often produced by spacecraft components. Thus, certain surfaces of spacecraft can experience a greater fluence of charged particles due to their proximity to on-board electromagnetic fields. Since droplets, transiting hundreds of meters, will only experience artificial magnetic fields when close to the

sending or receiving satellite, they will experience an unaltered flux of charged particles for the bulk of their transit time. This study does not consider the impact of on-board spacecraft magnetic fields and assumes that droplets are only affected by the unaltered ambient plasma environment.

The potential in the plasma near a charged surface V is given by the Poisson equation (equation 6).[16] The computer based charge simulation code; NASCAP solves this equation by applying the specified environment flux distribution electron and ion densities in an iterative process while developing the sheath at the surface and recalculating the particle densities accordingly. One advantage this gives NASCAP, over other charge modeling codes, is its ability to calculate accurate electric fields in the surrounding plasma.[21] NASCAP employs the Boundary Element Method as developed by Brebbia[23] as a means for relating fields and potentials in the surrounding plasma to sources at the surface. This method allows rapid determination of changes in plasma densities, current flow to/from the surface and a new solution to Poisson's equation to determine changes in electrostatic potential that occur during the time step. The time step is determined by the equation $\boldsymbol{\tau} = \boldsymbol{\Delta V j / c}$ where $\boldsymbol{j}$ is the maximum surface current density, $\boldsymbol{c}$ is the capacitance per unit area, and $\boldsymbol{\Delta V}$ is an approximate change in potential during the time step.[13]

Periods of minimum auroral activity have significant levels of electron flux at energies below 250eV where secondary electron production is high. However, even during minimum levels of auroral activity, the average energy of precipitating electrons is about 800eV and a significant portion of the incident electrons will cause deep bulk surface charging. During nominal conditions the average energy is 6000eV and during maximum auroral activity average the average energy state is 9000eV.

The high-energy state of auroral plasma beams implies that there is very little secondary electron production in both the nominal and maximum situations. Indeed, if the droplet presented a flat surface perpendicular to the beam the material would experience deep bulk surface charging almost exclusively. However, electrons with high incidence angles to the surface are more likely to produce secondaries that escape the material. As a result, it is expected that the hemisphere exposed to an auroral beam of electrons will have a more negative charge beneath surfaces that are more normal to the beam and a more positive charge on surfaces that are highly inclined to the beam. The worst-case scenario for maximizing droplet charge magnitude is one in which very few secondaries are emitted. Thus a droplet modeled as a flat surface positioned perpendicular to the auroral beam with primarily deep bulk surface charging will assume a conservatively negative floating potential. In the presence of low-energy plasma, such a strongly negative droplet will repel low energy electrons, and attract low energy ions present in auroral space.

Photons with wavelengths shorter than 165nm (1650 A) have a thermal energy greater than 7.5eV which is the threshold energy sufficient to eject measurable numbers of electrons from DC704 and DC705. This threshold energy was discovered by Koizumi, Lacmann and Schmidt[24] who looked at DC704 and DC705 photoelectron emissions involving the absorption of a photon, ionization of a silicon oil molecule, electron transport to the liquid/vacuum interface and escape into a vacuum. Incident photons are absorbed by a molecule of the liquid at distances between x and x+dx beneath the surface with a probability of $\mu\, e^{-\mu x}\, dx$, where μ is the photoabsorption coefficient.

In the Koizumi et al study,[24] a thin liquid film of DC705 and DC704 was applied to cathodes in vacuum and irradiated with ultraviolet light from a deuterium discharge lamp. The vacuum ultraviolet light was monochromatized and fell on the cathode through an anode mesh. Current induced by photoelectron emissions was measured as a function of photon energy. The relative light intensity was monitored by the fluorescence of Sodium Salicylate. Division of the current by the intensity of the fluorescence gave the relative photoelectron emission yield. The study looked at normal incidence of UV light on DC705 and DC704 and determined that the threshold photon energy required to liberate an electron for both fluids is 7.5 +/- 0.2 eV. The ratio of electrons released to photons absorbed (Y) peaks at about 73 electrons emitted for every 1000 photons and occurs at about 11eV incident photon energy (E_{photon}). The yield between 7.5 and 8.5 eV is roughly described by equation 7:

$$\boldsymbol{Y \propto (E_{photon} - 7.5)^3} \qquad \textbf{(7)}$$

Experimental results for DC704 and DC705 are indistinguishable from each other providing strong justification for the use of DC704 in photoemissions charging experimentation instead of the more costly DC705.[24]

Overlaying the nominal solar output with the quantum yield data as a function of wavelength instead yields the chart in Figure 9. This chart highlights the dramatic contribution of the Lyman Alpha spike in solar energy from the sun in the EUV part of the spectrum near 121.6nm (about 10eV). DC705 droplets in space due to photoemissions are dominated by these 10eV photons that produce a photoelectron yield of about 0.055.

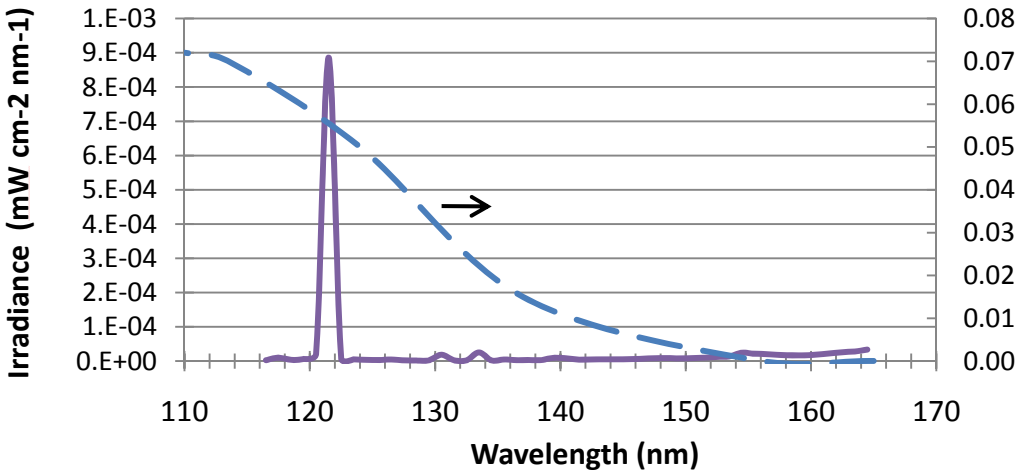

Figure 9. Nominal Solar Output (solid line) and Photoelectron Yield for Silicon Oil (dashed line plotted against the right ordinate).

D. Numerical Charging Simulations

Three professional charge modeling software tools were employed in this study to predict droplet charging. Results of these models were compared with each other and to analytic calculations to validate them to a first order approximation. The most powerful tool employed is NASA Charging Analyzer Program (NASCAP) ver. 3.2 developed by Science Applications International Corporation (SAIC) for the USAF and NASA. NASCAP considers geometry and numerous material properties allowing a charge prediction that is specific to non-traditional shapes and materials. The Maxwell probe formulation used by NASCAP to determine charge is, in principle, exact for a sphere in an isotropic, Maxwellian plasma.[25] Of particular importance to this study is NASCAP's ability to create materials by allowing the user to specify certain material properties.

The material properties used by NASCAP to model charging are shown in Table 3. Values for DC705 properties on the left side of the table were either provided by Dow Corning or found in the literature.[26,24,10] Values in the right half of the table were determined using theoretical equations, or estimated from Teflon properties. A parametric study was conducted to quantify the relative effect of each material in the right half of the table on droplet equilibrium charge as determined by NASCAP. Each property was varied by an amount within a reasonable range to quantify the impact on equilibrium surface charge reached in the GEO and auroral environments. Reasonable range of variation of each parameter was determined by researching properties for semi-conducting materials (typically Silicon) and insulating material (typically Teflon).

Dielectric constant is a measure of dielectric strength, which is the strongest electric field that can exist in a dielectric material before electrical breakdown (discharge) occurs. The dielectric constant of a material describes the factor by which the capacitance of two charged parallel plates changes when that material is used to fill the gap between the two plates. This is described by the following equation where $\boldsymbol{C_o}$ is capacitance with a vacuum separating the charged plates, $\boldsymbol{C}$ is the capacitance after insertion of the dielectric material, and κ is the dielectric constant specific to the dielectric material:[27]

$$\boldsymbol{C = \kappa C_o} \tag{8}$$

Similarly, voltage potential of the capacitor separated by vacuum is decreased by 1/κ when the dielectric material is inserted between plates as in the following relationship where V_o is the electrostatic voltage measured with vacuum separating two charged plates and V is the electrostatic voltage measured with the dielectric material between the charged plates.

$$V = \frac{V_o}{\kappa} \tag{9}$$

Bulk conductivity and density were identified in product literature and clarified through communications with a Dow Corning Applications Engineer.[iii] Both of these values vary slightly with temperature but varied less than 0.1% over the range of temperatures (200-350K) considered in this study. Simulations were performed to evaluate the effect of this slight variation in conductivity and density. These simulations show that slight variations in conductivity and density have no noticeable effect on equilibrium charge. The values of conductivity and density, listed in Table 3, were used for all simulations performed in this study.

Table 3. DC705 Material Properties Selected for Use by NASCAP.

Material Property	DC705 Value		Material Property	DC705 Value
Average Atomic Number	4.028		Maximum Secondary Yield due to Protons	0.455
Secondary Electron Maximum Yield (normal incidence)	2.0 electrons/electron		Energy of Maximum Secondary Yield due to Protons	140 eV
Maximum Photoelectron Yield (normal incidence)	0.073 electrons/photon		Surface Resistivity	$1x10^{16}$ ohms/m^2
Dielectric Constant	2.5		Range Coefficient	0.627
Thickness	Drop Radius (m)		Range Exponent	1.455
Bulk Conductivity	$1.0x10^{-12}$ $ohms^{-1}m^{-1}$			
Average Atomic Weight	7.583 amu			
Density	1097 kg/m^3			

Two thicknesses, 0.5mm and 4mm, were evaluated in both a GEO environment and in an auroral environment. Variation of material thickness had little effect on equilibrium charge in NASCAP simulations. This matched expectations since electron penetration range calculations predict electron penetration distance much less than a half millimeter in DC705 for energy states typical of electrons in near earth space. Once material thickness was determined to have little impact on charging, droplet radius was used for material thickness in simulations of spheres in this study. Material thickness of cubes was also varied with the same results as in spheres. Cube material thickness was set equal to half of the length of each side in cube simulations.

NASCAP assumes that the electron yield per photon is equal to the yield caused by normal incidence multiplied by the cosine of the angle of incidence to the sun (ψ_{sun}). Thus, the photocurrent from a surface exposed to the sun is given by the formula where i_{photo} is the current from the droplet surface to the ambient plasma. Y_{sun} is the normal incidence angle yield determined by Koizumi et al.[24] (a maximum of 0.073 electrons per photon for both DC-704 and 705).

$$i_{photo} = Y_{sun}\,(Area\ exposed)\cos\psi_{sun} \tag{10}$$

Two experiments were conducted in the study to quantify charging of silicone oil droplets that results from secondary electron production caused by photoemissions. Both experiments were carried out in a laboratory vacuum chamber and photoemission of electrons was accomplished by irradiation with an extreme ultraviolet (EUV) lamp. Droplet charge was measured and compared with levels predicted by NASCAP photoemission modeling of droplets. The main purpose was to validate photoemission charge modeling by NASCAP and to refine estimates of DC705 photoelectron yield. This property is used by NASCAP to predict current flow from a droplet due to electrons liberated by high-energy photons. A secondary goal of experimentation in this study was to devise a method of detecting stream impact location on a collector surface.

[iii] Private telephone conversation with Mr. James Wright, Applications Engineer, Dow Corning Corp. June 15, 2008.

Experimental results indicate that NASCAP droplet charging predictions of sunlit droplets, determined using a photoelectron yield of 0.073, are accurate to within 10% and are slightly conservative. This difference is small enough to conclude that 0.073 is appropriate to use in charging simulations and is slightly conservative for prediction of charge on both positively and negatively charged surface elements on sunlit spheres.[13]

The effect of photoemissions is graphically evident in NASCAP simulation results in shown in Figure 10. Here two drops are shown, the first in eclipse and the second in full sun with the sun in line with the x-axis. The legend to the right of the images shows that the eclipsed droplet exibits a nearly uniform negative potential of -15kV relative to the environment. The right droplet is exposed to sun on the right hemisphere which has a more positive charge potential than the shaded side. The sunlit droplet exibits negative charge on all of its surfaces but the surfaces normal to the sun have a potential 10kV more positive than those opposite the sun.

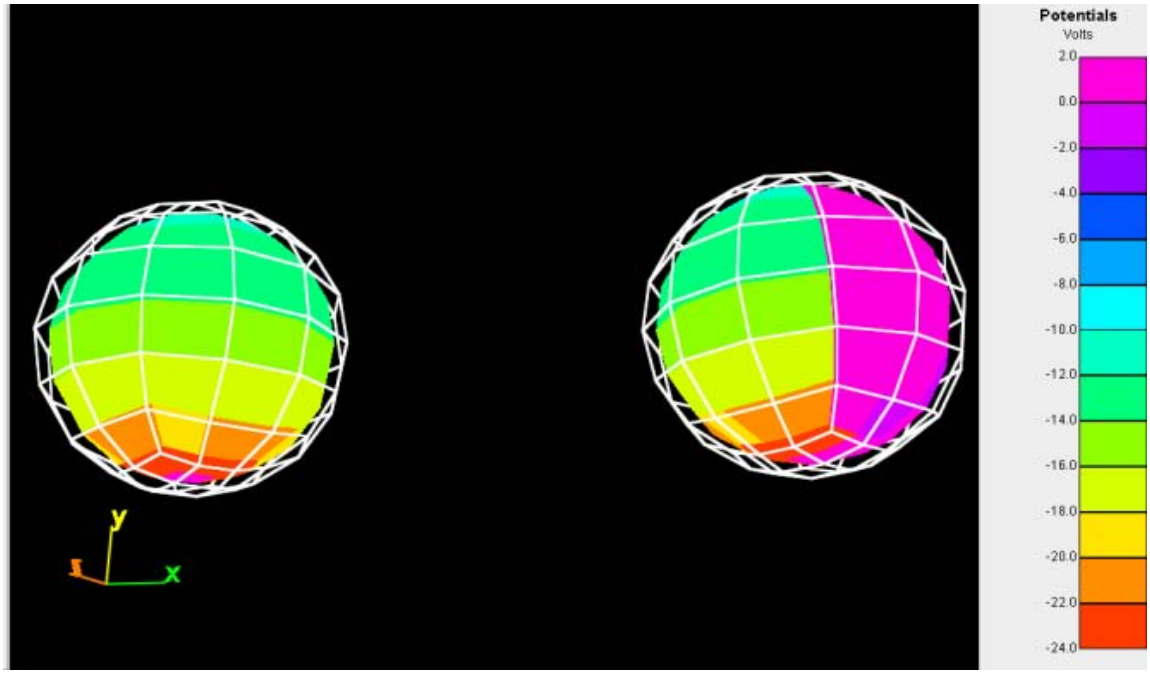

Figure 10. Comparison of Hemispheric Charging Impacted by Velocity and Solar Incidence.

Poisson's equation, which is the foundational equation that NASCAP solves to determine droplet charge, applies to matter in any state. However, NASCAP is not designed to account for the internal dynamics of a charged liquid. The liquid state has little effect at the atomic level where electrons are energized and ions created. At the inter-molecular level, like charges repel each other causing dilution of charge concentrations and a more uniformly distributed charge within droplets. In a sun-exposed droplet, this will likely result in negatively charged molecules migrating to the (more) positively charged sun-facing hemisphere. This migration will tend to mitigate the dipolar charging expected in sun-exposed droplets and lead to a more uniform charge distribution. Sunlit droplets are likely to have a charge distribution similar to that of droplets in eclipse but with a more positive overall charge. Droplets in eclipse will likely see a migration of charged droplets from the surface into the interior of the droplet resulting in a charge distribution more uniform throughout the sphere. The rate of migration depends on the level of charge and was not quantified in this study. Both of these charge distribution mechanisms support the assumption droplets can be treated as point charges when analyzing droplet interactions that affect their trajectory between satellites.

Once material properties of DC705 were identified for use in NASCAP, simulations were performed to evaluate droplets in different plasma environments. 8.3mm diameter DC705 spheres and 1.3mm cubes were simulated in isolation, as pairs and as strings of three. For LEO and Polar orbit simulations, velocity was usually assigned in the Y direction at 7.5 km/s and deviations from this practice will be noted. The sun vector was aligned with the X-axis in sunlit simulations presented in this report unless otherwise noted. A transit velocity of 20 or 100 m/s was assigned to the Z-axis in at least a dozen simulations but results showed no significant effect of this velocity on corresponding

ram or wake hemispheres. Orbital velocity is not considered in GEO simulations because of the slower orbital speed and the scarcity of low-energy positive ions that play a significant role in mitigating negative charge at lower altitudes.

In this study, NASCAP charging simulations of DC705 droplets in GEO were performed for nominal conditions and during high magnetospheric activity. These simulations show that droplet charging in GEO during nominal geomagnetic activity varies significantly from charging during peak geomagnetic activity. Nominal GEO charging results in positive surface potentials caused by secondary electrons produced by electrons with energy states between about 10 and 300eV. During high magnetospheric activity, the proportion of electrons with energy states above 300eV is much greater and negative deep surface charging processes dominate. Here, secondary electrons are created hundreds of Angstroms inside the material and, along with the incident electron, are absorbed by other molecules instead of escaping the material. This results in negative surface charging at a gradual rate, relative to rates in LEO.

It can take several minutes for droplets to reach equilibrium potential in GEO during high geomagnetic activity. Results of charging of a single 8.3mm DC705 droplet in the NASA Worst-case environment are shown in Figure 11. The chart includes results from simulations run in both eclipse and in sunlight. Sunlit surfaces in the chart below refer to the surfaces on the particular droplet most normal to the sun while anti-sun surfaces are those on the side of the droplet opposite the sun with the most negative charge potential. The plot shows the long period of time required to reach equilibrium charge in GEO during high geomagnetic activity. At reasonable transit speeds, droplets transiting spacecraft in GEO are unlikely to reach equilibrium potential before being collected. Droplets charged in the sun reach significantly more positive equilibrium charges than those in eclipse. The average charge of all surface elements on a sunlit droplet is about 75% less negative than the nearly uniform potentials reached by droplets in eclipse.

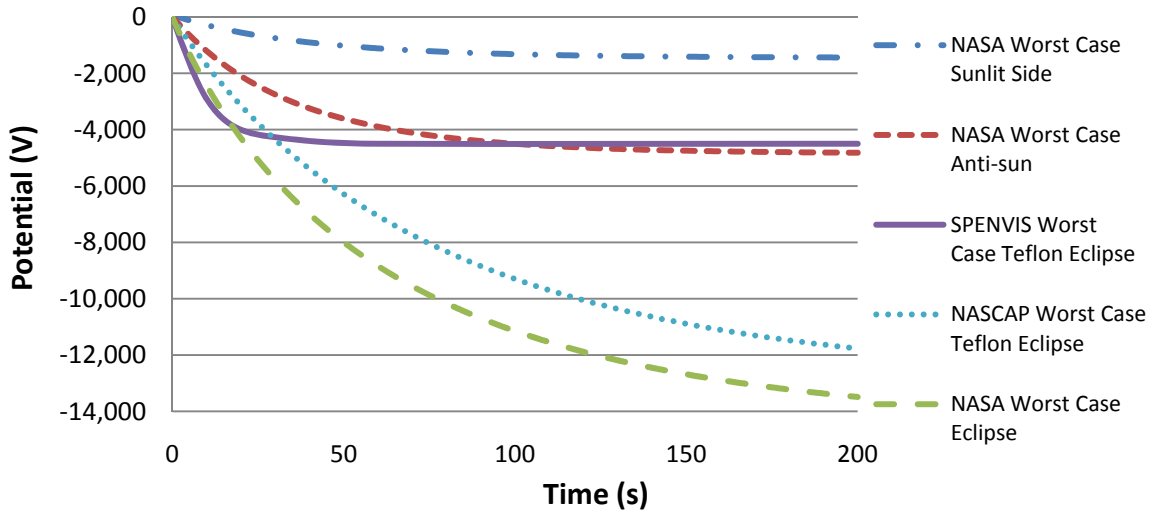

Figure 11. NASCAP Simulation of DC705 alongside SPENVIS and NASCAP Simulations of Teflon Spheres in Eclipse. All Simulations are in NASA's Worst-case GEO Charging Environment. In Sunlit Droplets, the Most Positive and Negative Potentials are found on the Sunlit and Anti-sun Surfaces, Respectively.

Teflon was simulated in strong GEO using NASCAP and the ESA charging model, SPENVIS to compare results with DC705 results. Surprisingly, both SPENVIS and NASCAP Teflon eclipse estimates are less negative than estimates for eclipsed DC705. This result is counter to the expectation that the strong insulator, Teflon, will charge more strongly than DC705, a semi-conductor. One explanation for the stronger charge potential seen in DC705 is lower density that allows greater electron penetration depth. This results in more pronounced deep bulk surface charging in DC705 than in Teflon. The most important finding of these simulations of high magnetospheric charging in GEO is that charge levels are above those at which droplet breakup occurs, even with very fast streams.

Because the atmospheric density is negligible at GEO altitudes and the magnetic field is very weak, the associated drag and electromagnetic interaction (Lorentz) forces are unlikely to affect the path of sub-droplets significantly. Electric fields between droplets in GEO during high magnetospheric conditions will be much stronger

than those in LEO. These forces can produce significant repulsion forces between droplets causing significant dispersion from the intended transit path.

Simulations of droplet charging in nominal GEO conditions show that droplets will charge positively on all surfaces with the maximum charge on any surface reaching about +20V. High magnetospheric activity as strong as the NASA Worst Case just described is rare, having occurred only a handful of times since the space age (and monitoring) began.[28] It typically takes 2-3 days for strong geomagnetic activity to dissipate, much longer than the 12 hours it takes for tandem satellites to merge following suspension of droplet streams. Magnetospheric events could also charge droplets to levels where Coulomb breakup occurs.[13]

Simulations of DC705 droplets in LEO reveal a charging environment that is more benign than the nominal GEO environment described in the last section. Shielding by Earth's magnetic field prevents most high-energy particles from reaching low latitude LEO. Charging of droplets in LEO is mitigated by low energy positive and negative ions (cool plasma) in the ionosphere. NASCAP simulations were run with multiple spheres in a nominal single Maxwellian LEO environment with electron and ion energy and density specified by the International Reference Ionosphere (IRI) for the orbit of the International Space Station (ISS).[29] In sunlight, DC705 spheres reach a very small, nearly uniform, negative charge potential of -0.01V relative to the ambient plasma in less than a second. In eclipse, the same LEO environment resulted in a surface potential of -0.05V. By comparison, NASCAP charging of a Teflon sphere in the eclipsed ISS environment resulted in a charge potential of -0.67V. Similarly, a charging simulation of an isolated Teflon patch in 300km low latitude LEO using SPENVIS resulted in an equilibrium potential of -0.80V. These results match expectations of a benign charge environment in LEO dominated by low-energy plasma. These low levels of charge are not expected to create any significant impediments to droplet stream operations.

Table 4 summarizes the results of more than a hundred NASCAP simulations of DC705 droplets in various environments. Shielding of high-energy particles by Earth's magnetic field and the presence of high numbers of low energy plasma particles makes low latitude LEO the most benign environment to operate in. Droplet charge potentials remain less than 2.1V despite high geomagnetic activity both in eclipse and in sunlight. The strongest charging is experienced in GEO where potentials can reach thousands of volts relative to surrounding plasma during high geomagnetic activity.

Table 4. Summary of Equilibrium Potentials (maximum sunlit surface and minimum eclipsed surface) and Time to Reach Equilibrium in the Environments Analyzed

Environment:	LEO	<800km Auroral (DMSP)	1500km Auroral (FREJA)	GEO
Low Geomagnetic	**+0V , -0.5V (sun, eclipse)**	**+1.5V, -2V**	**+2V, -14V**	**+18V, +1.5V**
Nominal Geomagnetic	**+0V , -1V**	**+4V, -16V**	**+6V, -25V**	**Not Analyzed**
High Geomagnetic	**+2V , -2V**	**+21V, -26V**	**Insufficient Data (3 years only)**	**-2kV, -13kV**

Analysis of auroral charging using environment data from DMSP spacecraft between 500 and 800km shows that charge will remain between -26V and +21V in and out of eclipse. Equilibrium potential is reached within 0.2 seconds without any significant overshoot of equilibrium potential in either sun or eclipse. Negative charging due to electron deposition and secondary electron production is rapid but is then mitigated by low-energy ions within half of a second. These levels of charge potential will affect droplet impact dispersion to a level quantified in the next section, along with methods of mitigation.

Sufficient Fontheim distribution data is not currently available to characterize the high auroral charging environment accurately during strong geomagnetic events. Droplet charging during moderate geomagnetic activity is characterized by rapid negative charging to magnitudes approaching those seen during strong charging events at lower altitudes. Photoemission charging of droplets in high auroral space is also rapid and results in spikes in voltage potential on all surfaces that are many times greater than the sunlit equilibrium charge but last just thousandths of a second. Further study of droplet charging in the high auroral environment is needed to accurately quantify negative charge potential during high magnetospheric activity.

G. Effect of Charge on Droplet Integrity and Motion

If droplets reach a high enough level of charge, coulomb repulsion forces within the droplet will overcome surface tension forces and the drop will break into smaller droplets.[30] The force of surface tension as a function of droplet radius, *r*, is described by the following equation:[26]

$$\boldsymbol{F_{surf\ tension} = 2\pi r\left(T_{surf}\right)} \tag{11}$$

where $\boldsymbol{T_{surf}}$ = 0.0365 N/m for DC705. If *Q* is the total charge of each hemisphere and $\boldsymbol{\varepsilon_0}$ is the permittivity constant of free space, Coulomb forces are described as a function of separation distance between volume centroids of each hemisphere:

$$\boldsymbol{F_c = {\varepsilon_0(Q_1Q_2)}/{r_{sep}^2}} \tag{12}$$

DC-705 droplets were analyzed for their potential to break apart when exposed to significant charge levels. Droplet charge can be expressed as a function of voltage potential and droplet capacitance. Capacitance is directly proportional to droplet diameter and charge is directly proportional to capacitance so, for a given equilibrium voltage potential, larger droplets have greater charge. However, larger droplets also have greater surface tension forces holding them together than smaller drops. The increase in surface tension force with size is greater than the increase in coulomb repulsion forces caused by the increase in droplet charge.

Larger droplets can withstand greater voltage potential before breaking up. Droplets with a relative potential of 300 volts that are smaller than a millimeter in diameter will tend to break apart. Since the maximum anticipated charge potential on droplet surfaces in <800km polar orbit is less than 26 volts, breakup of droplets due to electrostatic self-interaction is not likely in any low altitude orbits. The minimum DC705 droplet diameter required to prevent breakup at 26 volts charge potential is less than one micron (.0055 mm). Figure 12 shows a curve representing the point where coulomb forces and surface tension forces are equal as a function of droplet size and voltage potential. Droplets with diameters smaller than those corresponding to the curve will break up. It is evident that large droplets can withstand potentials of more than 1000 volts without breakup.

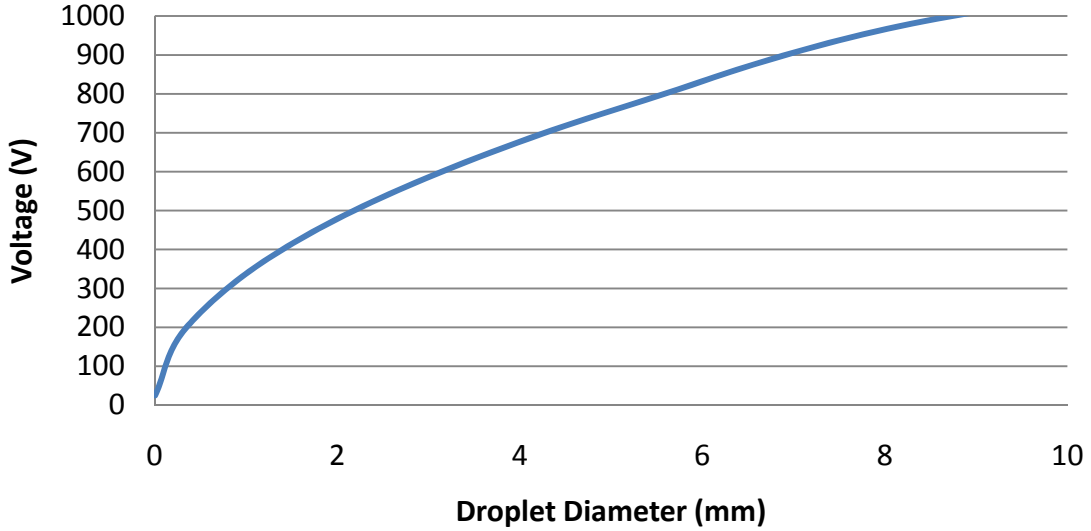

Figure 12. DC705 Droplet Breakup as a Function of Diameter and Voltage.

In GEO, voltage potential during strong geomagnetic activity is likely to reach the point where droplet breakup will occur. Droplet breakup results in sub-droplets of different size with different drag properties. At low altitudes, these sub-droplets are decelerated differently producing a large area of impact at the collection site. At GEO altitudes drag is negligible and sub-droplets can be collected, provided electric fields between droplets do not repel each other off course. It is shown in the next section that some uniformly sized droplets streams with small gap distances have an impact radius of more than a meter due to droplet e-field interaction. Electric field interactions between sub-droplets will be even more pronounced than interactions between uniformly sized droplets. This is

because of the relative mass difference between sub-droplets and because of their close proximity. Therefore, to avoid significant loss of fluid and possible spacecraft contamination, droplet streams in GEO must to be stopped prior to charge levels reaching the breakup point. This will probably require close monitoring of the charging environment with on-board sensors to stop droplet stream production if aspects of the local GEO plasma exceed certain thresholds. Since charging time in GEO can take several minutes, it may be possible to resume stream operations when spacecraft are closer. In this way, it may be possible to continue modified operations (and spacecraft cooling) and avoid collisions.

The magnetic field induced forces of principle concern to droplet stream propulsion is the Lorentz force which acts in accordance with the equation:[13]

$$\vec{\boldsymbol{F}} = \boldsymbol{q}\,(\vec{\boldsymbol{E}} + \vec{\boldsymbol{V}} \times \vec{\boldsymbol{B}}) \tag{13}$$

Here, $\vec{E}$ is any electric field present (in Newtons/Coulomb), $\vec{B}$ is any magnetic field present (in Teslas), $\vec{V}$ is the droplet velocity (in m/s) and q is the charge of the droplet (in Coulombs). In near Earth space, forces due to electric fields are at least an order of magnitude weaker than forces caused by Earth's magnetic field over the poles.[16]

The cross product of the droplet velocity $\vec{v}$ and magnetic field $\vec{B}$ results in a force acting perpendicular to both of these vectors. Because the primary Lorentz force acts nearly parallel to the path of transiting droplets, droplets are accelerated or slowed but the direction of droplet travel between satellites is altered very little. Lorentz forces are strongest in polar orbits where the strongest portions of Earth's magnetic field are encountered and the orbit velocity is nearly perpendicular to the magnetic field. Everywhere in a polar orbit, the vector between side-by-side satellites is perpendicular to the magnetic field lines. Over the geomagnetic equator, the orbit velocity is parallel to the magnetic field and Lorentz forces are nearly zero.

A polar orbit altitude of 300km was selected to analyze Lorentz force strength because it is near the lower limit of altitudes at which remote sensing satellites typically operate. The low altitude gives this orbit a relatively high orbit velocity and high magnetic field strength that result in high Lorentz forces. A 300km polar orbit is high enough that high-energy plasma can induce significant charging of droplets that transit between satellites as the spacecraft briefly passes through the auroral zones. Even in this worst-case orbit, Lorentz force strength will be quite weak. NASCAP modeling indicates droplet charge magnitude of more than 26 Volts below an altitude of 800km is unlikely even during periods of high geomagnetic activity. The Lorentz force acting on a 1mm droplet with a 26 volt potential is only 1×10^{-8} N. This small primary Lorentz force has little impact on the transit velocity of droplets. One stream is accelerated while the other is decelerated and the magnitude of acceleration is about a centimeter per second over a one-kilometer transit. A charge potential of 3300 Volts is required to completely stop a 1mm droplet launched at 20m/s before it travels 1km.[13]

An object with charge $\boldsymbol{q}$ exerts an electrostatic force on other charged objects that is equal to $\vec{\boldsymbol{F}} = \boldsymbol{q}\,\vec{\boldsymbol{E}}$. Here $\vec{\boldsymbol{E}}$ is the electric field produced by the object and the magnitude of $\vec{\boldsymbol{E}}$ is equal to the electrostatic potential of the object. In spherical objects that are charged uniformly and are of like charge $\vec{\boldsymbol{F}}$ is repulsive and acts along the line connecting sphere centers. A spherical Gaussian surface is applicable to finding the electric field outside of the sphere by a point charge or a uniformly charged spherical shell or any other charge distribution with spherical symmetry.[31] Gauss' law, which is one of Maxwell's equations of electromagnetism, can be expressed as:

$$\oint_0^{\boldsymbol{S}} \boldsymbol{E}\cdot\boldsymbol{dA} = \frac{\boldsymbol{q}}{\boldsymbol{\varepsilon_0}} \tag{14}$$

where $\boldsymbol{E}$ is the electric field strength, the vacuum permittivity constant $\boldsymbol{\varepsilon_0}$ = 8.854e-12 $C^2N^{-1}m^{-2}$, and $\boldsymbol{dA}$ is a differential surface area. $\boldsymbol{S}$ is a Gaussian surface, chosen so that it is concentric to and outside of the droplet surface enclosing the uniformly distributed charge $\boldsymbol{q}$. By the assumption of spherical symmetry, the integrand is a constant ($4\pi r^2$) and can be taken out of the integral resulting in:

$$\boldsymbol{4\pi r^2\hat{r}\cdot\,E(r)} = \frac{\boldsymbol{q}}{\boldsymbol{\varepsilon_0}} \tag{15}$$

where $\hat{\boldsymbol{r}}$ is a unit vector normal to the surface. Because the charge is symmetric within the sphere, $\boldsymbol{E}$ also points in the radial direction, and is then equal to:

$$\vec{\boldsymbol{E}}(\boldsymbol{r}) = \frac{\boldsymbol{q}}{\boldsymbol{4\pi\varepsilon_0\,r^2}}\hat{\boldsymbol{r}} \tag{16}$$

Thus, Coulomb's law quantifies the electric field strength emanating from a charged droplet:

$$\boldsymbol{E(r)} = \frac{\boldsymbol{q}}{\boldsymbol{4\pi\varepsilon_0 r^2}} \tag{17}$$

The electrostatic potential (Coulomb potential) of an isolated sphere with charge $\boldsymbol{q}$ at a distance from the center, $\boldsymbol{r}$ is then:

$$\boldsymbol{\psi(r)} = \boldsymbol{q}/\boldsymbol{4\pi\varepsilon_0 r} \tag{18}$$

Droplets in eclipse acquire a charge (usually negative) that is nearly uniform and therefore will produce electric field forces that repel each other. Sunlit droplets acquire positive charge on the sun facing side for a brief period before taking on a negative, or less positive, charge that remains less negative than the side opposite the sun. In most cases, uniformly charged droplets in eclipse represent the worst-case scenario for amplification of droplet angular dispersion because repulsion forces between droplets are strongest. Sunlit droplets are more positively charged on the sun-facing hemisphere and therefore have weaker repulsion forces than droplets that are uniformly charged, as they are in eclipse. The one exception to this rule, found in this study, is a sunlit droplet in GEO with nominal geomagnetic conditions.

Secondary electron production in GEO nominal geomagnetic conditions causes droplets to take on a positive charge, even in eclipse. Such a droplet can have a sunlit hemisphere with up to +20V potential and an anti-solar side charged to no more than +2V. Because strongly charged hemispheres must face the sun, it is not possible for any two +20V hemispheres to face (and therefore repel) each other. Thus, the worst-case repulsion in GEO nominal geomagnetic conditions results in a repulsion force comparable to that of two eclipsed droplets each uniformly charged to less than 7 volts. Since this force is less than that produced by droplets in several eclipsed environments the droplet repulsion between sunlit droplets was not analyzed in this study.

A numerical model was developed to simulate the effect of electric field interactions between droplets transiting over a user specified distance. This code serves as a tool to analyze the impact of various droplet stream parameters such as charge, stream velocity, and droplet spacing on required collector size. The model takes droplet diameter, spacing, angular dispersion, velocity dispersion and charge potential as inputs and simulates droplet production and the three dimensional motion of droplets transiting a specified distance. The model then provides the impact location and distance from centerline and calculates a standard deviation of droplet dispersion from centerline.

Without charging, the dispersion of droplet impact from centerline follows a normal distribution centered at the vector between satellites. 5000 simulated uncharged droplets impacted no more than 3mm from the collector's center after 50 seconds of travel. This dispersion conforms to a normal distribution with the standard deviation of angular dispersion from stream centerline equal to values determined by USC researchers using DC704 droplet streams.**Error! Bookmark not defined.**

When droplets are uniformly charged electrostatic dispersion from stream centerline results in a ring shaped impact region at the droplet collector like the one depicted in Figure 13. The impact ring shown was created by simulating the transit of 1000, two-millimeter droplets each charged to 100V potential. The circle depicted in the figure has a radius that is three standard deviations from centerline, large enough to collect 99.7% of transiting droplets. By choosing an acceptable percentage of collected droplets, a corresponding standard deviation can be determined and the collector sized accordingly. For the example shown, a collector 60cm in diameter fails to collect about 30 droplets in 5 years while a 70cm collector only loses one droplet in 5 years.

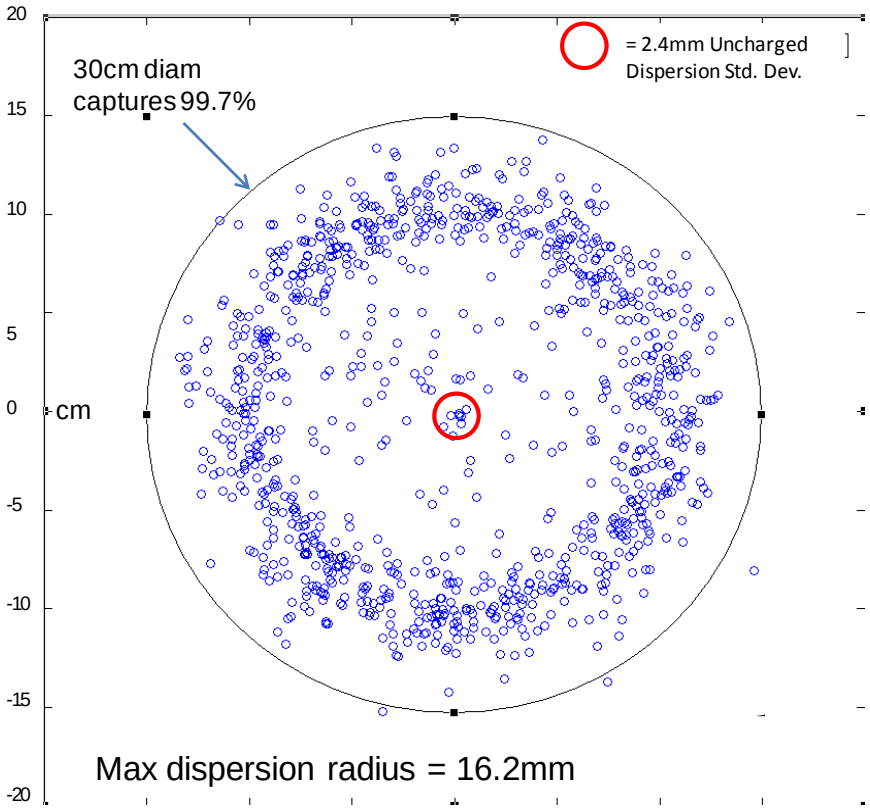

Figure 13. Charged Droplet Impact Point for 2mm Droplets after 50 second Transit

Stream parameters affecting dispersion include velocity, charge potential, droplet spacing, and droplet diameter. Increased velocity decreases dispersion by reducing the time droplets have to repel each other and then translate from centerline during transit. Since the electrostatic force between droplets decreases with the square of the distance the effect of droplet spacing was analyzed by simulating three different droplet diameters produced with various gap to diameter ratios between 1/3 and 3. Each droplet simulated had a voltage potential of 100V, a stream speed of 29m/s, and a transit distance of 1km. Maximum miss distance of any droplet in each simulation is shown in Figure 14. At each droplet size the expected trend of decreasing miss distance with increasing gap distance is confirmed. Power law trend lines, applied to the data set for each droplet diameter indicate that the relationship between droplet miss distance and gap length becomes more linear as droplet diameter is increased.

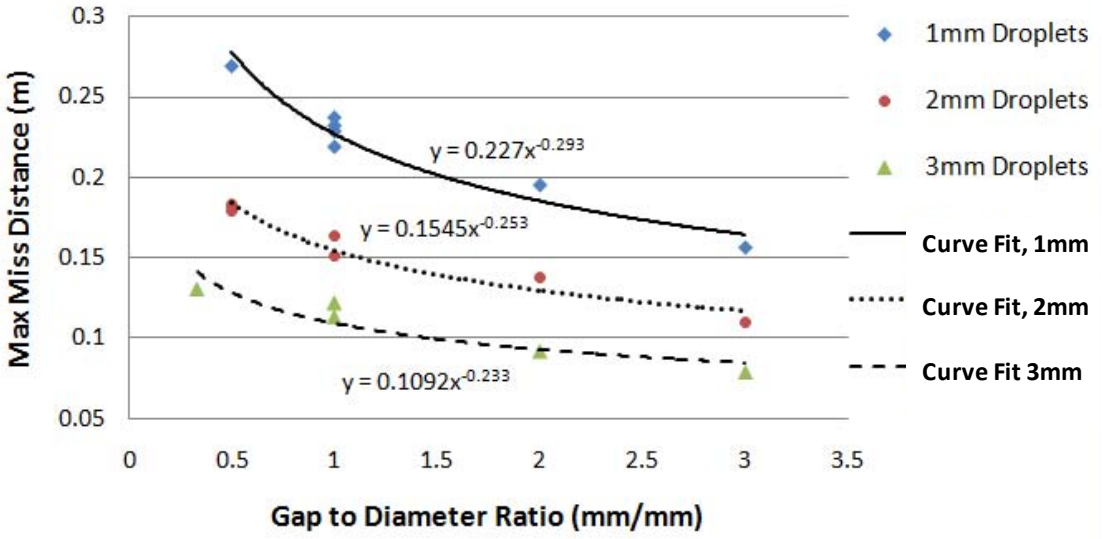

Figure 14. Results of Transit Simulations with Different Gap Distances between Droplets. Power Law Curve Fits to Simulation Data indicate an Inverse Relationship between Maximum Miss Distance and Droplet Diameter.

A simulation of transiting droplets with voltage potentials near that predicted by NASCAP was performed to predict off-course drift of droplets operating in an auroral environment. A 2mm diameter and 2mm gap distance stream transiting at 29m/s and charged to a 30V potential was simulated and maximum miss distances recorded. These miss distances were compared with those of an identical stream charged to 100V. The 100V stream had a maximum miss distance of 15.1cm while the 30V stream maximum miss distance was only 4.7cm. The same simulation of 30V droplets was performed with 1mm and 3mm droplets and yielded similar comparisons between 100V dispersion and 30V dispersions.

At potentials expected below 800km in auroral space, simulations of transiting charged droplets show that droplet drift is limited to less than about 5cm. The fact that the impact location of droplets conforms to a ring pattern complicates the collection of droplets since multiple droplet impacts at the same site may be required to overcome adherence to the collector surface and acceleration of the captured fluid to the collection site. Another simulation was performed in which gap distance between 2mm diameter, 30V droplets was increased to 8mm. The 4 to 1 gap to diameter ratio resulted in a decrease in the one-sigma impact ring diameter from about 10cm down to about 6cm. Using solenoid valve droplet generator technology even longer gaps are possible, allowing effective mitigation of droplet dispersion due to inter-droplet interactions. Not accounted for, in these simulations, is plasma damping of electrostatic potential between droplets caused by sheath formation around each droplet. Such damping decreases the repulsion forces between droplets therefore droplet dispersion simulation results are slightly conservative.[13]

III. Conclusions

Analyses of various aspects of the droplet stream propulsion concept show it is sound and at least an order of magnitude more efficient than high Isp electric propulsion systems at performing the same tandem satellite mission. A droplet stream system weighs about one-fifth as much as a comparable ion engine and consumes about 1000 times less power. The relatively low required operating power of droplet stream propulsion effectively makes it an enabling technology for side-by-side tandem formation satellites. In addition, a droplet stream propulsion system contains most of the components needed in a Liquid Droplet Radiator (LDR). Such a radiator is more efficient than conventional radiators on a mass basis and its use offsets the mass of conventional thermal control system mass in most satellites. Many components such as collectors and pumps were developed and tested as part of the LDR program and are well suited to droplet stream propulsion with only minor modifications.

In this study, charging of DC705 droplets in space was analyzed with numerical methods for the first time. More than 200 simulations were performed using carefully researched material properties and environmental parameters. Simulation results presented in Chapter 3 indicate that, under nominal geomagnetic conditions, transient and equilibrium droplet potential is less than 10V relative to the ambient plasma in the LEO, auroral, and GEO environments. During periods of high geomagnetic activity auroral space can charge droplets to potentials approaching -30V. Strong geomagnetic activity may induce strongly negative levels of charge in droplets in GEO and possibly in high auroral space. Analysis in Chapter 4 shows that charge can reach thousands of volts in GEO during high magnetospheric activity and can induce droplet breakup as Coulomb forces overcome surface tension. Charging events of this magnitude are expected every 8-11 years. Droplet charging is slow in GEO and short transits limit the amount of charge acquired, preventing Coulomb breakup of droplets. Short transits also minimize off-course drift of charged droplets caused by interactions with other charged droplets or sub droplets. Lorentz forces will cause polar orbiting droplets to accelerate in a direction perpendicular to both the orbital velocity and Earth's magnetic field. For polar orbiting tandem satellites, this acceleration of droplets is primarily in a direction that will increase or decrease transit speeds. Lorentz force acceleration is small compared to droplet acceleration due to drag or electric fields and is unlikely to 124 affect the required collector size significantly. In GEO and low-latitude LEO, Earth's magnetic field is much weaker and Lorentz force accelerations are insignificant relative to other forces acting on droplets.

References

[1]Zink, M., Krieger G., Fiedler H, Moreira L. The TanDEM-X Mission: Overview and Status. Proceedings of the Geoscience and Remote Sensing Symposium, 2007. IGARSS 2007. IEEE International 23-28 July 2007 Page(s): 3944 - 3947

[2] Tragesser, S. Static Formations Using Momentum Exchange Between Satellites. AIAA/AAS Astrodynamics Specialist Conference, August 18-21, 2008.

[3] Sandau, R., H. Röser and A. Valenzuela. Small Satellites for Earth Observation. Springer Press, Netherlands © 2008.

[4] White, K. Liquid Droplet Radiator Development status, AIAA Paper 87-1537, June 1987.

[5] Mattick, A., A. Hertzberg. Liquid Droplet Radiators for Heat Rejection in Space. Journal of Energy 5 (6) (1981) 387–393.

[6] Muntz, E., M. Dixon, Applications to Space Operations of Free-Flying, Controlled Streams of Liquids. Journal of Spacecraft, Vol. 23, No. 4, July-August 1986.

[7] Grumman Aerospace. Liquid Droplet Radiator Collector Component Development AFRPL TR-85-082, 1985.

[8] Pfeiffer, S. Conceptual Design of Liquid Droplet Radiator Shuttle-Attached Experiment. Grumman Space Systems, NASA Contract Report 185165, October 1989.

[9] Totani, T., Kodama, T., Nagata, H., Kudo, I., Thermal Design of Liquid Droplet Radiator for Space Solar-Power System. Journal of Spacecraft and Rockets, Vol. 42, No. 3, May-June 2005.

[10] Issikawa, K., K. Goto. Secondary Electron Emissions from Diffusion Pump oils I. Japanese Journal of Applied Physics, Vol. 6, No. 11, November 1967.

[11] White, F. Fluid Mechanics. 6th Ed. McGraw Hill, © 2009.

[12] Tagliafico, A., M. Fossa. Liquid Sheet Radiators for Space Power Systems. Proc Instn Mech Engrs Vol 213 Part G. © 1999

[13] Joslyn, T. Charging Effects on Fluid Stream Droplets for Momentum Exchange Between Spacecraft. PhD Dissertation, University of Colorado, Colorado Springs, Nov 18, 2009.

[14] EADS Astrium Corp. Space Propulsion Website: www.cs.astrium.eads.net/sp/ [accessed Sep 29, 2009].

[15] Dumke, M., T. Tombrelloa, R. Wellerb, R. Housleyc and E. Cirlinc, Sputtering of the Gallium-indium Eutectic Alloy in the Liquid Phase. Surface Science. Volume 124, Issues 2-3, Jan 2, 1983. Pg. 407-422.

[16] Chen, Francis. Introduction to Plasma Physics. Harper Press, Chicago, © 1984.

[17] Purvis, C., H. B. Garrett, A. C. Whittlesey, N. J. Stevens, Design Guidelines for Assessing and Controlling Spacecraft Charging Effects, NASA TP 2361, 1984.

[18] Garrett H., A. Whittlesey. Spacecraft Charging Requirements and Engineering Issues. ©AIAA, 2005.

[19] Tribble, A. The Space Environment. Princeton University Press, © 1995.

[20] Chen, F., R. Huddlestone (ed.) Plasma Diagnostic Techniques. Academic Press, New York, 1965

[21] Hastings, D., Garrett, H., Spacecraft Environment Interactions. Cambridge University Press. © 1996.

[22] Garrett, H. and C. Pike, ed. Space Systems and Their Interactions with Earth's Space Environment. Progress in Astronautics and Aeronautics, Vol 71. AIAA. 1980.

[23] Brebbia, S. Boundary Element Methods, Springer Verlag, New York, 1981.

[24] Koizumi, H., S. Lacmann, Light-induced Electron Emission from Polymethylphenyl Siloxane Oils. IEEE Transactions on Dielectrics and Electrical Insulation, Vol. 3 No. 2, April 1996, pg. 233.

[25] Katz, I., D. Parks, M. Mandell, J. Harvey, D. Brownell, Jr., S. Wang, M. Rotenberg, A Three Dimensional Dynamic Study of Electrostatic Charging in Materials, NASA CR 135256, 1977.

[26] Dow Corning Technical Library. Available online. http://www.dowcorning.com. [Accessed Nov, 2009].

[27] Serway, R. Physics for Engineers and Scientists. 2nd Edition. Saunders College Pulishing. ©1986.

[28] NOAA SPACE ENVIRONMENT SERVICES CENTER:Solar Proton Events Affecting the Earth Environment, Preliminary Listing, 1976 – present. Online: http://umbra.nascom.nasa.gov/SEP/seps.html [Accessed Jun, 2009].

[29] NASA Goddard Earth Sciences Data and Information Services Center GES DISC, http://disc.sci.gsfc.nasa.gov/ [Accessed Feb, 2009].

[30] Pickett, G. Presentation online: Self Assembly of Charged Polymers 2008. Department of Physics and Astronomy, California State University Long Beach. http://www.csulb.edu/~gpickett/PhysicsSDSU.pdf [Accessed Jan, 2009].

[31] Tipler, P. and M. Gene, Physics for Scientists and Engineers (Extended Version) (5th ed.). W.H. Freeman Press, © 2004. ISBN 0-7167-4389-2.